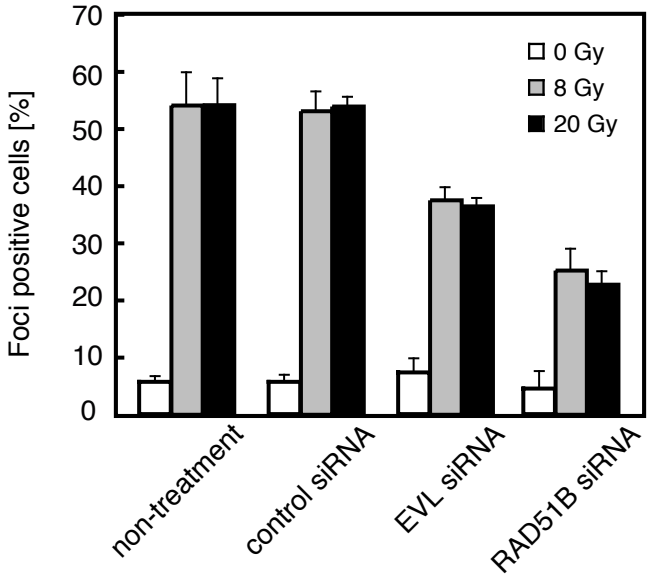

Supplementary Fig. 1. **RAD51-foci formation.** Graphic representation of the RAD51-foci formation after γ-ray irradiation (8 and 20 Gy). The cells containing more than ten RAD51 foci were scored as positive, and were plotted. The averages of three independent experiments are plotted with SD values. Defects in the RAD51-foci formation in MCF7 cells were detected after 20 Gy irradiation, as well as after 8 Gy irradiation.

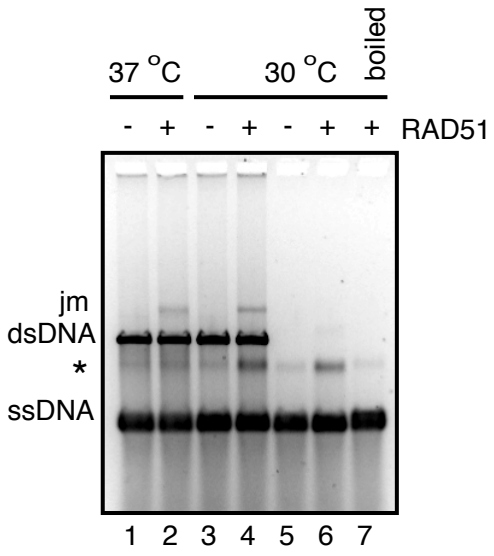

Supplementary Fig. 2. **Partial annealing products of ssDNA detected in the RAD51-mediated strand-exchange assay at 30°C.** Lanes 1 and 2 indicate experiments at 37°C, and lanes 3-7 indicate experiments at 30°C. Lanes 1, 3, and 5 represent experiments without the RAD51 protein. A small amount of the ssDNA self-annealing product was observed in the absence of the RAD51 protein, suggesting it is not produced by incomplete deproteinization. Lanes 5-7 represent experiments without dsDNA. Self-annealing products were also detected even in the absence of dsDNA, and were resolved by heating. Therefore, we conclude that the products were actually partial annealing products of ssDNA.

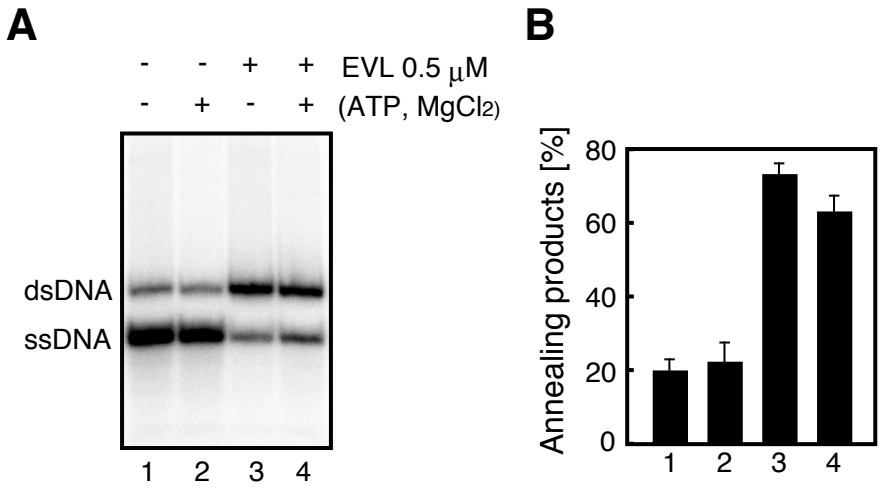

Supplementary Fig. 3. **Effects of ATP and $MgCl_2$ (1 mM) on the EVL-mediated annealing reaction.** (A) Lanes 1-2 indicate negative control reactions without the EVL protein, and lanes 3-4 represent experiments with the EVL protein. Lanes 1 and 3 represent experiments in the absence of ATP and 1 mM $MgCl_2$. Lanes 2 and 4 represent experiments in the presence of ATP and 1 mM $MgCl_2$. The EVL protein concentration was 0.5 μM. (B) Graphical representation of the experiments shown in panel A. The band intensities of the annealing products were quantified. The averages of three independent experiments are plotted with SD values.